DAYLIGHT ELECTROLUMINESCENCE IMAGING METHODOLOGY COMPARISON

Gisele A. dos Reis Benatto[1], Thøger Kari[1], Rodrigo Del Prado Santamaria[1], Sergiu V. Spataru[1], Cristian Terrados[2], Diego González-Francés[2], Julián Anaya[2], Kabir Sulca[2], Victor Gómez-Alonso[2], Miguel Ángel González[2], Oscar Martínez[2]
[1]Department of Electrical and Photonics Engineering, Technical University of Denmark (DTU), Frederiksborgvej 399, 4000 Roskilde, Denmark.
[2]GdS-Optronlab group, Dpto. Física de la Materia Condensada. Universidad de Valladolid. Edificio LUCIA. Paseo de Belén, 11. 47011 Valladolid, Spain.

ABSTRACT: Electroluminescence imaging is a powerful technique for PV fault diagnosis and for this reason there is a growing interest of the O&M industry to make it widely available for in site inspections instead of randomly choosing samples throughout the PV plant. Few groups in the world disclose methodologies for daylight EL (dEL) image acquisition of installed PV modules, using different equipment and image processing procedures. In this work, we aim to compare methodologies from two research groups that have been working on practical ways to perform robust dEL imaging in parallel. We present the results from acquisitions made with similar but not identical equipment, weather conditions and PV module technologies. Image processing on the same datasets from both laboratories is performed using their own methods, indicating if the image processing methods and approach provide consistent results or not. While each laboratory has developed its own signal-to-noise ratio markers, both present good consistency with signal at an exposure time analysis, but not always a direct correspondence to the image quality. This intercomparison will lead to improvements on each laboratory procedure, expand the discussion to other groups and initiate a discussion on the establishment of dEL image quality and SNR metric baselines.
Keywords: Daylight electroluminescence, PV modules, PV reliability.

1 INTRODUCTION

Electroluminescence (EL) is often used as ground truth for detection defects in PV modules and cells thanks to its characteristics of detecting a wide range of faults and high spatial resolution [1]. Nighttime EL doesn't provide major challenges, but there's still a big interest in performing it during daytime, as it assures accessibility and safety in dealing with high voltage equipment and cabling. Only a few groups worldwide have the capability for daylight EL (dEL) image acquisition of installed PV modules using different equipment and image processing procedures, and even less of them have described methodologies in publications [2]–[4].

Currently, there's no agreement or standard for dEL practices, making the development of the technique challenging in terms of robustness for different weather conditions and other (possibly unknown) factors. This work should pinpoint key considerations for robust dEL imaging and establish pathways for a future interlaboratory comparison of image processing and experimental methods aiming the best outcome for automatic power output assessment based on EL images [5], [6].

2 METHODOLOGY

2.1 Experimental details

To achieve and evaluate the methods for dEL imaging, here we compare the experimental data that were performed by two research laboratories, one located at the Technical University of Denmark (DTU) and another at the University of Valladolid (UVa). At DTU, the current bias was applied using an Electro-Automatik PSI 9000 DC power supply unit (PSU). At UVa, the module is powered by the PSU Electro-Automatik 91500-30 3U, which can generate DC voltages up to 1500 V and currents up to 30A, as long as 15000 W is not exceeded. Different types of waveforms can be programmed in both power supplies such as square, sinusoidal, or triangular waveforms, and even an arbitrary shape can be programmed by software. For this work square and sinusoidal current bias waveforms of different frequencies have been selected. The current amplitude was set to oscillate from 0 A to ~ I_{SC} for both waveforms and at both laboratories. DTU and UVa used multi-crystalline silicon Aluminum Back Surface Field (Al-BSF) modules (60 cells and 72 cells respectively) as devices under test for a low EL signal scenario. Additionally, modules with higher open circuit voltage solar cells (Passivated Emitter and Rear Contact - PERC) were also used for a high EL signal scenario. In this case, DTU used a monocrystalline silicon PERC module and UVa a multi-crystalline PERC. The same type of cells in the compared modules should assure that the EL signal magnitude is equivalent when the same current bias is applied to them. Particularly, Al-BSF modules represent the most demanding scenario since the EL signal has the lowest luminescence emission from the large-scale commercially available PV module.

The dEL image sequences were acquired using SWIR cameras equipped with 640x512 InGaAs sensors and with 600 frames per second maximum frame rate. Both laboratories had available similar cameras from First Light Imaging: a C-RED 3 camera is used by DTU while UVa uses a C-RED 2 Lite camera. For all image data to be more efficiently used by the image processing method developed by DTU, the number of images per current bias modulation period at the PV module to be even, and particularly for the Fast Fourier Transform (FFT) method it was advantageous that the sequences had 8 images minimum per period, as it is shown in Fig. 1. Besides this ratio requirement expressed by equation (1) to be equal to 8, there's no type of active synchronization between the camera and the PSU.

$$\#\ of\ images\ per\ period = \frac{Frame\ rate}{Modulation\ frequency} \quad (1)$$

10.4229/EUPVSEC2023/4CV.1.7
020374-001

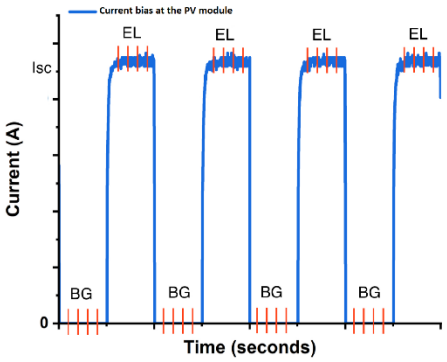

Figure 1: Current bias from a squared wave modulation (blue line) with 8 images acquired per period: 4 background images (BG) and 4 EL images.

As an exception, image sequences acquired with 2 ms exposure times had 16 images per period, to make better use of the high framerate available on the C-RED cameras. If this requirement is fulfilled, the DTU image processing method should provide its best results, even though the processing can also be performed when the requirement is not fulfilled. For the UVa processing method, this requirement also helps but is not a strict condition.

2.2 Image processing and signal-noise ratio (SNR) metric

For dEL, it is worth mentioning that the image processing is attached to the acquisition method itself, and this is also one of the important points of this laboratory intercomparison.

From the DTU side, the dEL images were processed with software developed in-house, which can use several different image processing methods. One of them used at this work was FFT, which generates a signal-to-noise ratio marker SNR_{Kari} [7]. A satisfactory signal for image extraction was extracted when $SNR_{Kari} = 1$ and upward. Values of $SNR_{Kari} > 4$ ensured a high-quality image, while values below one resulted in poor quality [7]. The software can process the images using a prevailing method found in the literature called Lock-in method which is described in detail by Adam et. Al. [8] which is an analysis made on time domain, opposing FFT which is a frequency domain analysis. For the Lock-in, a SNR marker SNR_{AVG} is reported in the literature [2], [3], [7], [9], which has been proven to present many inconsistencies in being an efficient signal and image quality metric [2], [7].

At UVa, the images are processed using two different methods: Frequency Domain (FD) and Time Domain (TD). In FD, image sequences acquired with both sinusoidal and square modulation waveforms can be processed, while for TD, only square waveform acquisitions can be considered. The SNR value for FD is calculated from the peak amplitude at modulation frequency and the variance of the noise level as:

$$SNR = \begin{cases} 10log_{10}\left(\frac{(Peak\ amplitude)^2}{Var(Noise)}\right) & if > 10 \\ 0 & if \leq 10 \end{cases} \quad (2)$$

where the peak amplitude is defined as the difference between the value at excitation frequency and the average of the [f/2,2f] \{f} window, and the variance is calculated also in the [f/2,2f] \{f} window, both calculated from the absolute value of the FFT resultant frequency domain data. Here 10 dB is defined as the minimal SNR to recognize that the signal can be distinguished from the noise level, which roughly corresponds to a peak signal ~3 times higher than the standard deviation of the noise level. Finally, the quality metric is the average SNR of the pixels with SNR values in the lower quartile (SNR_{25}), i.e. those with the weakest SNR. Therefore, the higher that value the better we can distinguish the weakest part of the image from noise.

For TD, the SNR value is calculated from average difference between the *On* and *Off states* and the variance of the noise level as:

$$SNR = \begin{cases} 10\,log_{10}\left(\frac{(On_{avg} - Off_{avg})^2}{Var(Noise)}\right) & if > 3 \\ 0 & if \leq 3 \end{cases} \quad (3)$$

Here 3 dB is defined as the minimal SNR to recognize that the signal can be distinguished from the noise level, which corresponds to roughly ~92% certainty that the pixel signal has been modulated by the external waveform. For satisfactory image quality $SNR_{25} > 15$dB should be the indication for this marker when FD is used and a $SNR_{25} > 5$ dB when TD is used.

In principle, the FFT and FD can be considered equivalents, dealing with the EL signal extraction on the frequency domain, the same way that TD and Lock-in image processing method interpret the signal in time domain.

3 RESULTS COMPARISON AND DISCUSSION

At this section, the qualitative image quality is evaluated comparing examples of image sequence acquisitions from both groups with different image processing methods and modulation waveforms performed by DTU (section 3.1) and UVa (section 3.2). Quantitative comparison of the SNR markers is made for different exposure times and module technologies in section 3.3.

3.1 DTU image processing method

In Fig. 2, the comparison between similar experiments performed at DTU and UVa is shown using squared and sinusoidal waveform current bias modulation. In Fig. 2 and Fig. 3, the exposure time is given in milliseconds (ms), framerate in frames per second (fps), current bias modulation frequency in hertz (Hz) and approximate solar irradiance in the plane-of-the-array (POA) at the time of the measurement in watts per square meter (W/m^2). For the DTU experiment, FFT image processing for dEL method presents slightly better quality than Lock-in- for both waveforms. The dEL resulting images clearly show major cracks and electrically isolated areas, but only the FFT processed may present similar image quality as the indoor EL image which is the reference for the quality to work for automatic defect detection algorithms. For UVa data, Lock-in shows better results, but neither of the processing methods show high quality images similar to the indoor data. Regarding the SNR markers indication, SNR_{Kari} is higher than 1 for both measurements, but the image quality itself might not be enough for proper diagnosis evaluation even from an inspector. The marker does show higher values for the square waveform, and the image quality is also better in the same way.

3.2 UVa image processing method

Fig. 3 shows the dEL images from sequences acquired at UVa and DTU with current bias modulation using different waveforms, compared with their indoor EL images (same indoor images as in Fig. 2).

10.4229/EUPVSEC2023/4CV.1.7
020374-002

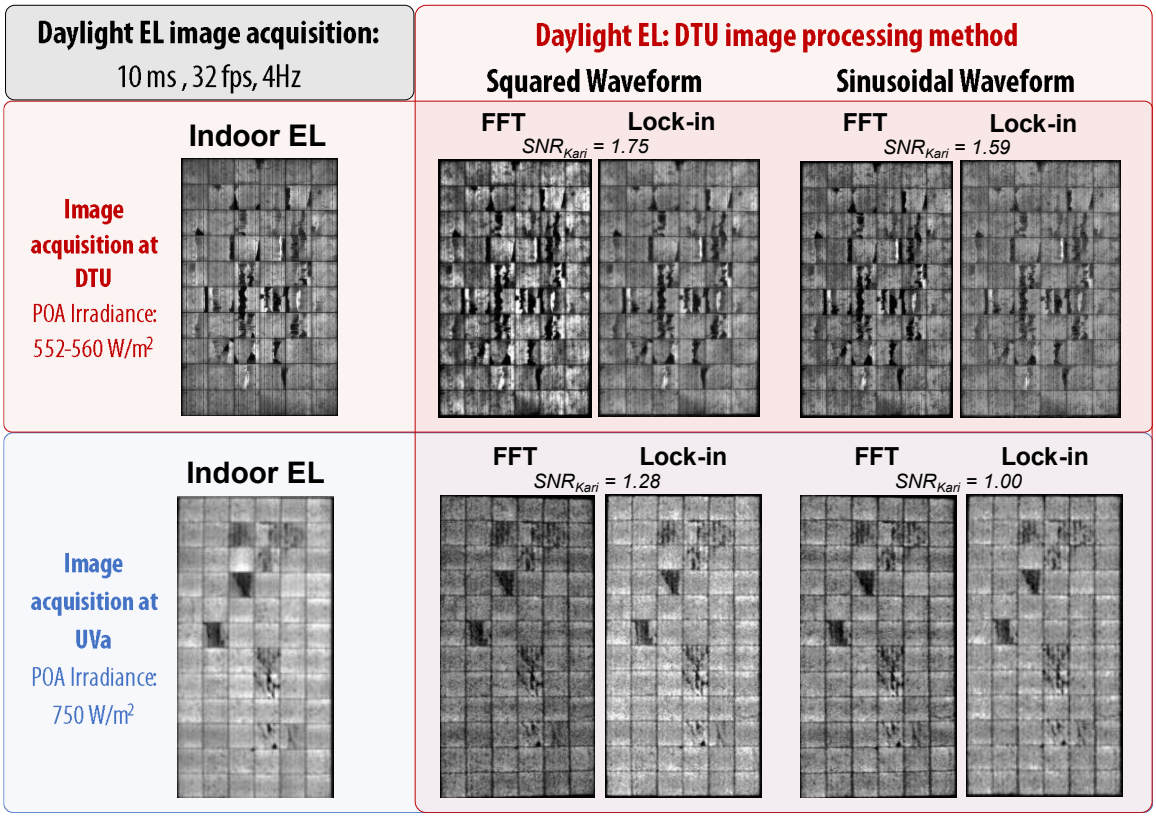

Figure 2: Indoor EL and dEL images acquired at both laboratories and processed by DTU's image processing method.

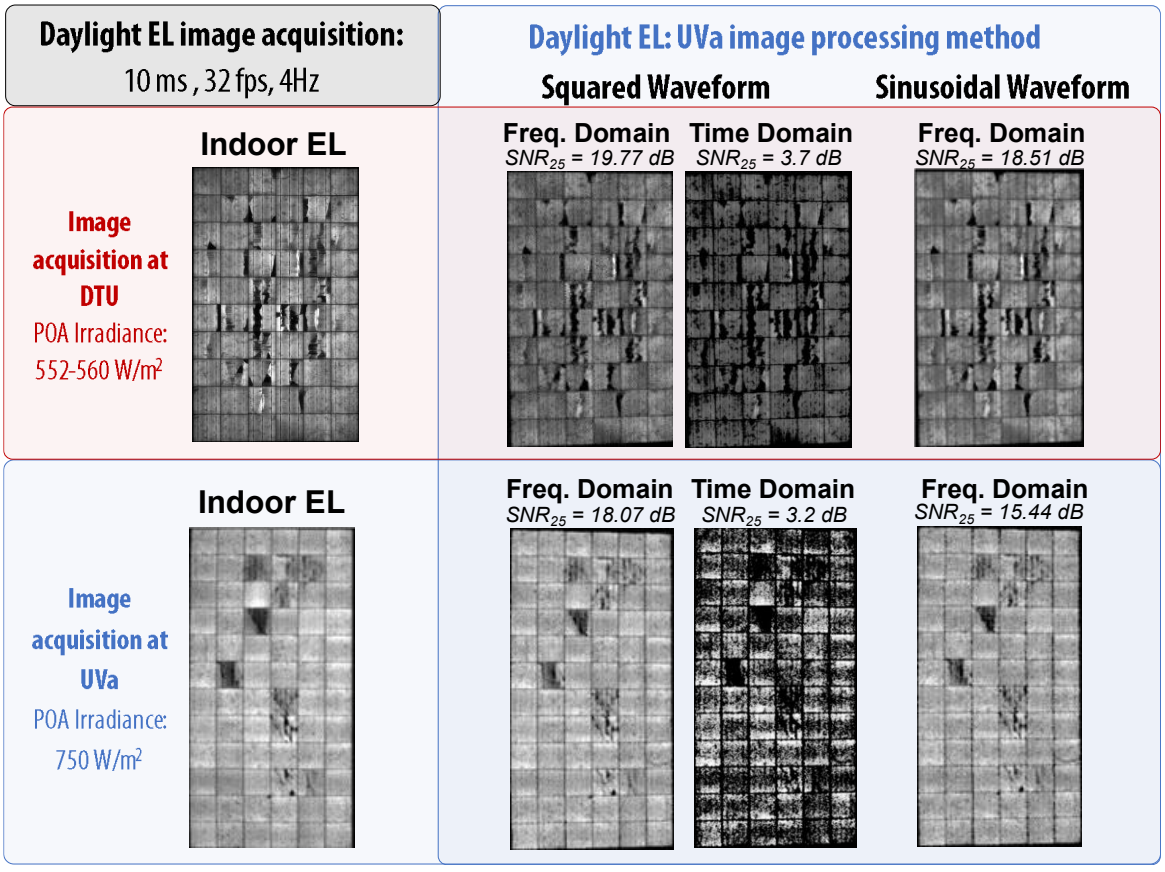

Figure 3: Indoor EL and dEL images acquired at both laboratories and processed by UVa's image processing method.

10.4229/EUPVSEC2023/4CV.1.7
020374-003

better contrast and similar quality as the indoors EL image. For the DTU data, both waveforms resulted in almost identical dEL images, however both with lower contrasts and sharpness than the indoors EL image. The SNR_{25} marker presents satisfactory values, although UVa dEL image with sinusoidal waveform may not be considered satisfactory qualitatively due to excessive granularity. For TD image processing, possible to be run for the square waveform, the dEL images quality was inferior to FD, with SNR_{25} equal to 3.2 and 3.7 dB for UVa and DTU data respectively, which were below the SNR_{25} good quality threshold.

3.3 SNR markers

The need to have an SNR marker that indicates quantitatively the quality of dEL images is paramount for large-scale automatic image quality evaluation, development of efficient image processing methods and understanding of the environmental factors that contribute in different proportions to generate noise during image sequence acquisition.

As observed in previous studies [2], [7] the first SNR marker for dEL mentioned in the literature SNR_{AVG}, presents high level of inconsistencies, having high values for low quality images at low exposure time (i.e. low signal), and low values for high quality dEL images. Fig. 4 and 5 show how the newer markers SNR_{Kari} and SNR_{25} perform with exposure time and different module technologies.

As mentioned previously, Al-BSF modules present a low EL signal due to its lower open circuit voltage compared to newer silicon cell technologies; therefore, it is the most challenging crystalline silicon PV module to perform dEL. For such modules, the dEL image processing method in general provided markers with good correspondence to exposure time and therefore with the amount of EL signal. It's worth noting that square waveforms tend to yield slightly better results compared to sinusoidal waveforms. In the case of the UVa processing, this seems to be related to the fact that the sinusoidal excitation is very weak in some frames of the cycle to contribute to the FFT, while the square excitation tends to be better resolved in its dominant frequency.

For strong EL emission PERC modules, the markers' correlations with exposure time seems to be consistent especially for the square waveforms, and for the UVa image processing, for the TD type. However, we observe a worsening of the SNR_{25} with the exposure time for the FD analysis that is related to the presence of light coming from reflections on the terrain surface. It should be noted that these panels emit EL intense enough to illuminate the scene, resulting in a weak modulated light coming from regions outside the panel. Since UVa is not cropping the images to the panel region only but keeping the whole 640 x 512 pixels from the camera, the increased exposure time leads to the inclusion of more weakly illuminated pixels

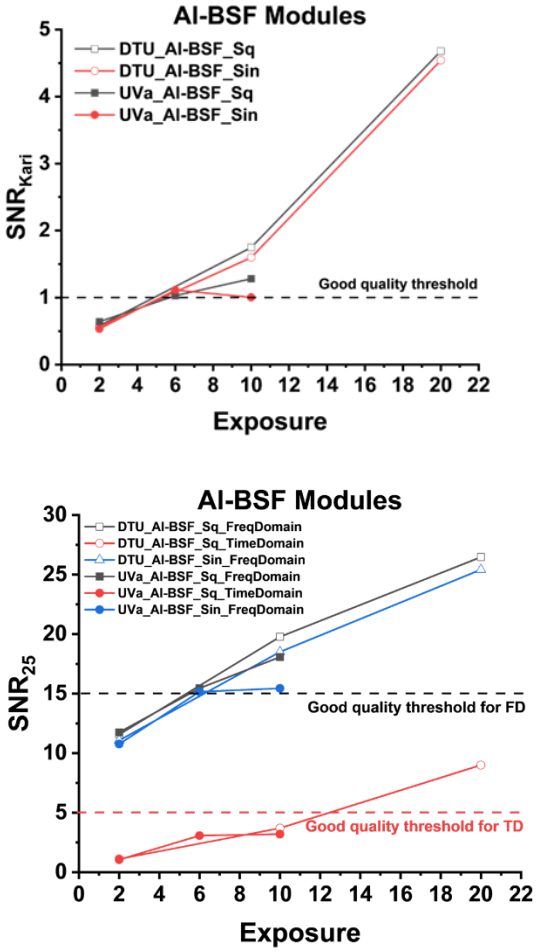

Figure 4: SNR_{Kari} and SNR_{25} markers for dEL images of Al-BSF modules for different image current bias waveforms and exposure times.

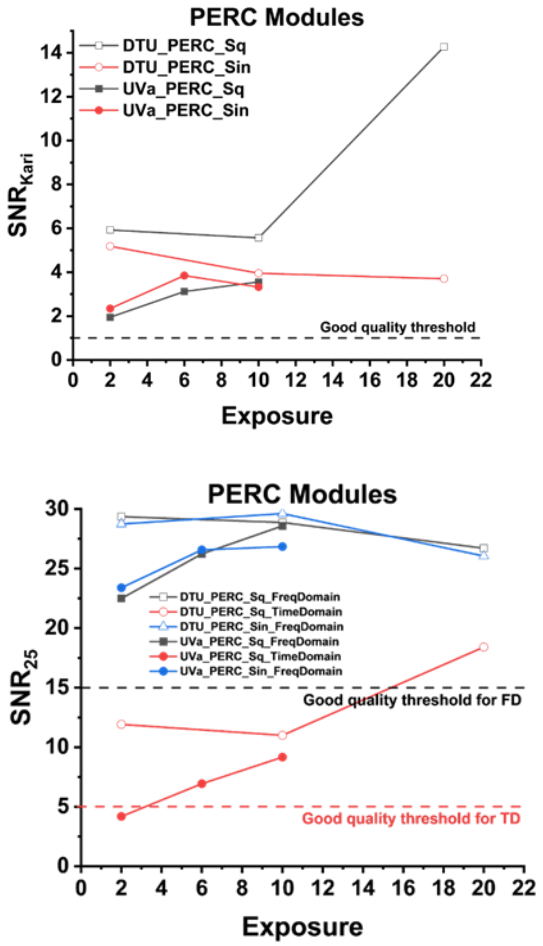

Figure 5: SNR_{Kari} and SNR_{25} markers for dEL images of PERC modules for different image current bias waveforms and exposure times.

10.4229/EUPVSEC2023/4CV.1.7
020374-004

from outside the panel area. Consequently, the SNR_{25} deteriorates in the 20 ms exposure case compared to the 10 ms case due to the increased presence of weak pixels outside the panel. The same effect is reasonable to be also occurring for SNR_{Kari} in the case of the sinusoidal waveform and for the square waveform at 10 ms exposure time.

This phenomenon is not observed in the case of the Al-BSF panels, as their emission is not intense enough to significantly illuminate the scene and be detected as a signal. Therefore, increasing the exposure time results in improved image quality markers for these panels.

In the context of the TD analysis, which is less sensitive to capturing modulated light from the panels, it cannot effectively distinguish the reflected light outside of the panels beyond the 3 dB cutoff limit. As a result, we do not observe the deterioration of SNR_{25} with increasing exposure time in the TD analysis.

4 CONCLUSIONS

In summary, both SNR marker approaches are more consistent for square waveforms than for sinusoidal. This same trend is also observed in the quality of the images, where frequency domain approaches (FFT and FD) is the more efficient to generate a dEL for qualitative evaluation of the PV modules health.

The SNR metrics appear to show consistent trends with exposure time, which hints at predictability. These deviations are internally consistent, and the experimental reasons can mostly be traced back and explained. Yet, when compared to each other, the image quality between laboratories cannot have a proper quantitative measure due to the different SNR marker definitions, bringing up again the problem of only relying on the observation of the dEL image by a human to define if a processing method is better or worse than the other.

For automated processing, the results of this intercomparison underline the paramount importance of establishing an SNR metric for dEL imaging that can be used universally and is robust for different approaches of image processing.

This intercomparison will lead to improvements on laboratory procedures, expand the discussion to other groups, and lay the groundwork for future round-robin discussions, intended for comparison of experimental practices, image processing approaches, and most importantly the establishment of dEL image quality and SNR metric baselines for daylight luminescence.

5 ACKNOWLEDGEMENTS

The UVa group has been financed by the Spanish Ministry of Science and Innovation, under project PID2020-113533RB-C33, and by the Regional Government of Castilla y León (Junta de Castilla y León) and by the Ministry of Science and Innovation and the European Union NextGenerationEU / PRTR under the project "*Programa Complementario de Materiales Avanzados*". The DTU group is supported by the Eurostars project Automated Daylight Electroluminescence Inspection of Large Photovoltaic Systems (ADELI).

6 REFERENCES

[1] L. Koester, S. Lindig, A. Louwen, A. Astigarraga, G. Manzolini, and D. Moser, "Review of photovoltaic module degradation, field inspection techniques and techno-economic assessment," *Renew. Sustain. Energy Rev.*, vol. 165, no. November 2021, p. 112616, 2022, doi: 10.1016/j.rser.2022.112616.

[2] G. Alves Dos Reis Benatto *et al.*, "Drone-Based Daylight Electroluminescence Imaging of PV Modules," *IEEE J. Photovoltaics*, vol. 10, no. 3, pp. 872–877, 2020, doi: 10.1109/JPHOTOV.2020.2978068.

[3] M. Guada *et al.*, "Daylight luminescence system for silicon solar panels based on a bias switching method," *Energy Sci. Eng.*, no. June, pp. 1–15, 2020, doi: 10.1002/ese3.781.

[4] T. J. Silverman, M. G. Deceglie, K. Vansant, S. Johnston, and I. Repins, "Illuminated Outdoor Luminescence Imaging of Photovoltaic Modules," *IEEE Photovolt. Spec. Conf.*, 2017.

[5] T. Kropp, M. Schubert, and J. H. Werner, "Quantitative prediction of power loss for damaged photovoltaic modules using electroluminescence," *Energies*, vol. 11, no. 5, 2018, doi: 10.3390/en11051172.

[6] R. del Prado Santamaría, T.K. Hass, G. A. dos R. Benatto, J. W. Ng, P. B. Poulsen, and S. V. Spataru, "Machine Aided Estimation of Solar Cell Crack Caused Power Loss from Electroluminescence Images," in *8th World Conference on Photovoltaic Energy Conversion*, 2022, pp. 480–487. doi: 10.4229/WCPEC-82022-3BO.11.6.

[7] G. A. dos Reis Benatto *et al.*, "Daylight Electroluminescence of PV Modules in Field Installations: When Electrical Signal Modulation is Required?," in *8th World Conference on Photovoltaic Energy Conversion*, 2022, pp. 735–739. doi: 10.4229/WCPEC-82022-3BV.3.44.

[8] J. Adams *et al.*, "Non-Stationary Outdoor EL-Measurements with a Fast and Highly Sensitive InGaAs Camera," *32nd Eur. Photovolt. Sol. Energy Conf. Exhib.*, 2016.

[9] C. Mantel *et al.*, "SNR Study of Outdoor Electroluminescence Images under High Sun Irradiation," in *2018 IEEE 7th World Conference on Photovoltaic Energy Conversion (WCPEC) (A Joint Conference of 45th IEEE PVSC, 28th PVSEC & 34th EU PVSEC)*, Jun. 2018, no. 1, pp. 3285–3289. doi: 10.1109/PVSC.2018.8548264.